Precision Photonic Readout for Focal Plane Signals

August 1999

Geert Wyntjes*, Alex Newburgh, Thomas Hudson**

Visidyne, Inc.
10 Corporate Place
South Bedford Street
Burlington, MA 01803

Abstract

We will present the development of a remote Precision Photonic Readout for Focal Plane Array Detectors. Its underlying principles, design and tests as well as limitations will be discussed. The design, in essence, constitutes a remote, via fiber optics, analog-to-digital converter, where the low level focal plane signals are encoded as differential optical phase shifts. These phase shifts are then recovered as digital numbers at a location external to the detector dewar.

The input transducer, a waveguide modulator is electrically passive with a response, which is absolute and unaffected by temperature. The design also provides for nearly complete EMI immunity and appears to be tolerant to radiation effects. As presently comprised it can satisfy the requirements of resolution, precision, bandwidth and dynamic range for all existing Focal Plane Imagers, as well as for future ones under development. Its small size, negligible mass and minimal heatload contribute to its use where these factors are important. We present quantitative data supporting these points, as well as visible and IR Imagery, which were obtained and transmitted off the focal plane by a prototype design.

* Author to whom all communication should be addressed.
E-mail: wyntjes@visidyne.com

** Stewart Radiance Laboratory/Utah State University Research Foundation, Bedford. MA

Background

The cryogenically cooled Infrared Focal Plane Arrays (IRFPA's) produce large bandwidth (Mpixels/sec), small (picowatt, nanovolt) signals. During their transmission from the dewar cold finger to the warm outside world for further processing they are highly susceptible to Electro Magnetic Interference (EMI). This susceptibility has impaired a number of critical missions [1]. A number of efforts to minimize the perils of EMI such as the Mosaic Array Data Compression and Processing (MADCAP)[2] scheme have been initiated. MADCAP proposes to address the issue of EMI by moving the processing electronics, Analog-to-Digital Converters (ADC's), Digital Signal Processing (DSP) chips to or near the FPA. The

Form SF298 Citation Data

Report Date *("DD MON YYYY")* 00081999	**Report Type** N/A	**Dates Covered (from... to)** *("DD MON YYYY")*

Title and Subtitle Precision Photonic Readout for Focal Plane Signals	**Contract or Grant Number**
	Program Element Number
Authors	**Project Number**
	Task Number
	Work Unit Number
Performing Organization Name(s) and Address(es) Visidyne, Inc. 10 Corporate Place South Bedford Street Burlington, MA 01803 &	**Performing Organization Number(s)**
Sponsoring/Monitoring Agency Name(s) and Address(es)	**Monitoring Agency Acronym**
	Monitoring Agency Report Number(s)
Distribution/Availability Statement Approved for public release, distribution unlimited	
Supplementary Notes	
Abstract	
Subject Terms	
Document Classification unclassified	**Classification of SF298** unclassified
Classification of Abstract unclassified	**Limitation of Abstract** unlimited
Number of Pages 12	

processed signals would then be transmitted as a high rate digital bit stream. This requires specialized chip designs and packaging techniques to operate at reduced temperatures, and in addition would increase the heatload on the dewar while potentially causing EMI of its own. An effort to overcome the low temperature limits of the electronics using superconducting elements for the electronics, has been sponsored by BMDO at JPL and TRW[3]. However, one potential problem appears to be a serious impedance mismatch between the FPA and the superconducting ADC.[4] A natural solution in light of the success of optical, analog and digital communication networks is to consider an optical method of transmission through the modulation of an optical carrier by the FPA signal. In fact, a number of attempts to design such a capability have been made. They have either been based on the direct current modulation of a laser diode intensity with the signals from the FPA[5] or indirect intensity modulation using an interferometric device in the form of a Mach-Zehnder (MZ) interferometer implemented as an a optical waveguide.[6] Both these approaches, while having sufficient bandwidth, fall short in terms of resolution and precision since both these modulation processes are inherently non-linear, affected by operating point stability and suffer from added noise due to relative laser intensity noise (RIN). A solution Visidyne has chosen is to modulate the phase of the optical carrier by varying the optical path difference between two optical beams through a strictly linear electro-optical process. Once the beams are outside the dewar, the FPA signals are recovered as a binary weighted digital representations of the original signal.

Phase Modulated Optical Link

The overall concept for a precision phase modulated optical link is illustrated in Figure 1. The voltage from the IRFPA detector is applied, with or without additional amplification, gain *G*, to a balanced pair of optical waveguide modulators. These sustain a single polarization and spatial mode, and are commonly implemented on a $LiNbO_3$ crystal substrate. They are physically small, < 1" long, and a few mm wide. The applied voltage introduces a path difference of approximately 125 nanometers per volt, or for a wavelength of $\lambda = 800\ nm$, a signal voltage of approximately *3.4 V* will introduce a phase shift of ≈ 400 nm or $\lambda/2$, half a cycle, π radians, a value often called V_π. An optical fiber fed pair, driven in push-pull configuration, would then require a voltage of $V_{\pi\ for}$ a full cycle of phase shift, 2π. One advantage of waveguide modulators lies in their low heat dissipation due to their very high impedance. In addition, the modulator response is strictly linear with applied voltage (see inset of Figure 1), over many cycles of phase, up to the breakdown voltage limit of at least 10 cycles. The modulator remains nearly instantaneous in their signal response for frequencies greater than 3 GHz.

As outlined in Figure 1, the light from a small laser diode external to the dewar is brought in by a single mode fiber, and equally divided into the two arms of the waveguide modulator. Two exit fibers then bring the two output beams having the differential phase shift $\phi = V \cdot G / V_\pi$ to an outside interferometer/receiver after which a digital phase processor recovers the phase shift as a digital representation $\Phi = \phi_{min}^{2(n-1)} + 2^{(m-1)}$, where the first term to the right of the equation, ϕ_{min}, represents the fractional phase and the second term the number of whole cycles. Typically the minimally resolvable phase value approaches $\phi_{min} = 10^{-4}$ cycles and a bandwidth of > 10 MHz in an optimized configuration. The phase value phase is equivalent to a path difference resolution of approximately 80 pm. The second term is usually limited to 1 to 2 cycles, for a total dynamic range of 2×10^4 (≈ 13 bits, or 78 dB). The key difference between this approach and those cited previously, is instead of carrying the signal information as in intensity modulation, the information is carried as a differential phase shift between two optical beams, carriers. The fundamental advantage of modulating the phase, is that the signal phase is independent of the received light level, power on the receiver, including those due to changes in laser

output and fiber losses. This is because the phase is recovered as a ratio between two signals and is not affected by laser intensity noise making it possible to reach shot noise limited sensitivity down to very low frequencies.

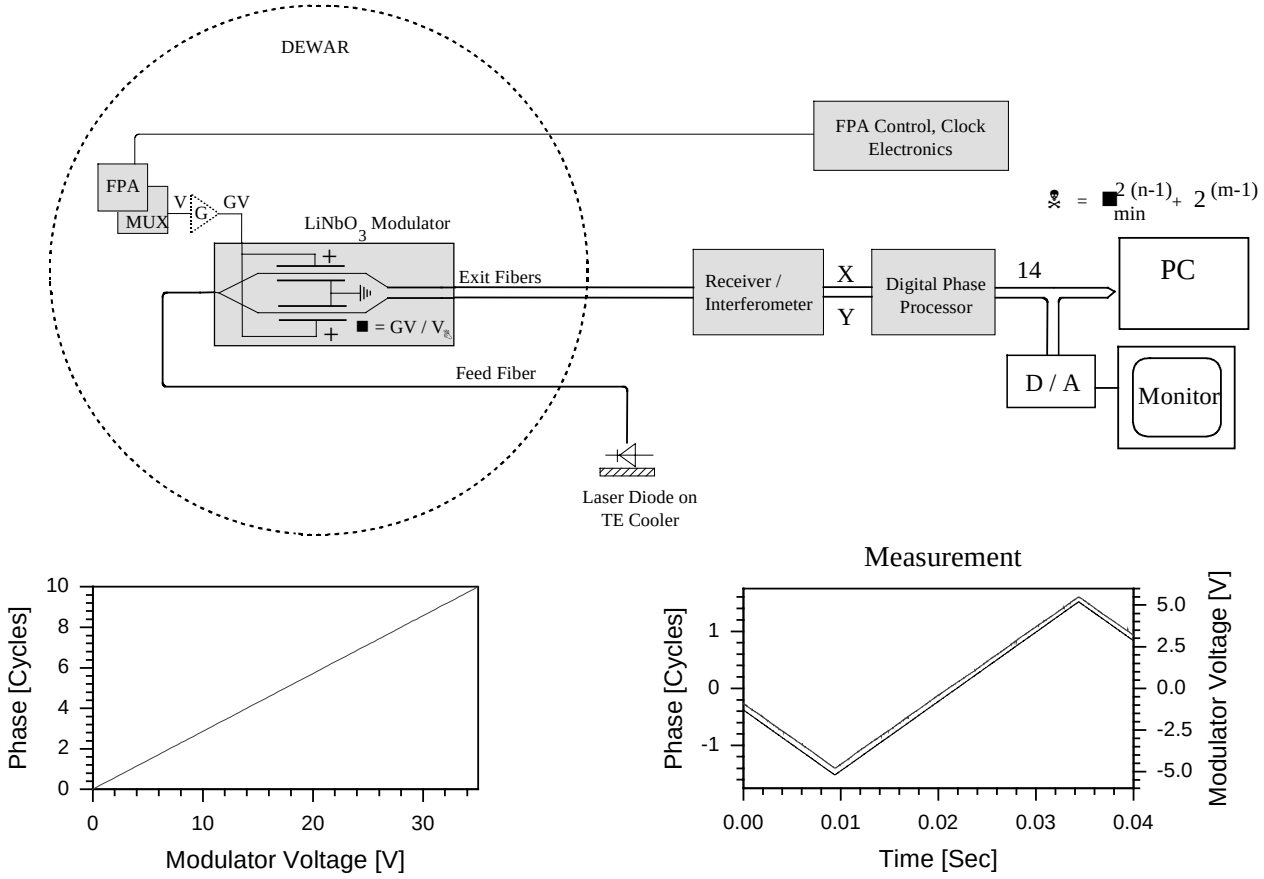

Figure 1: The Cryogenic Optical Link (Cryolink)

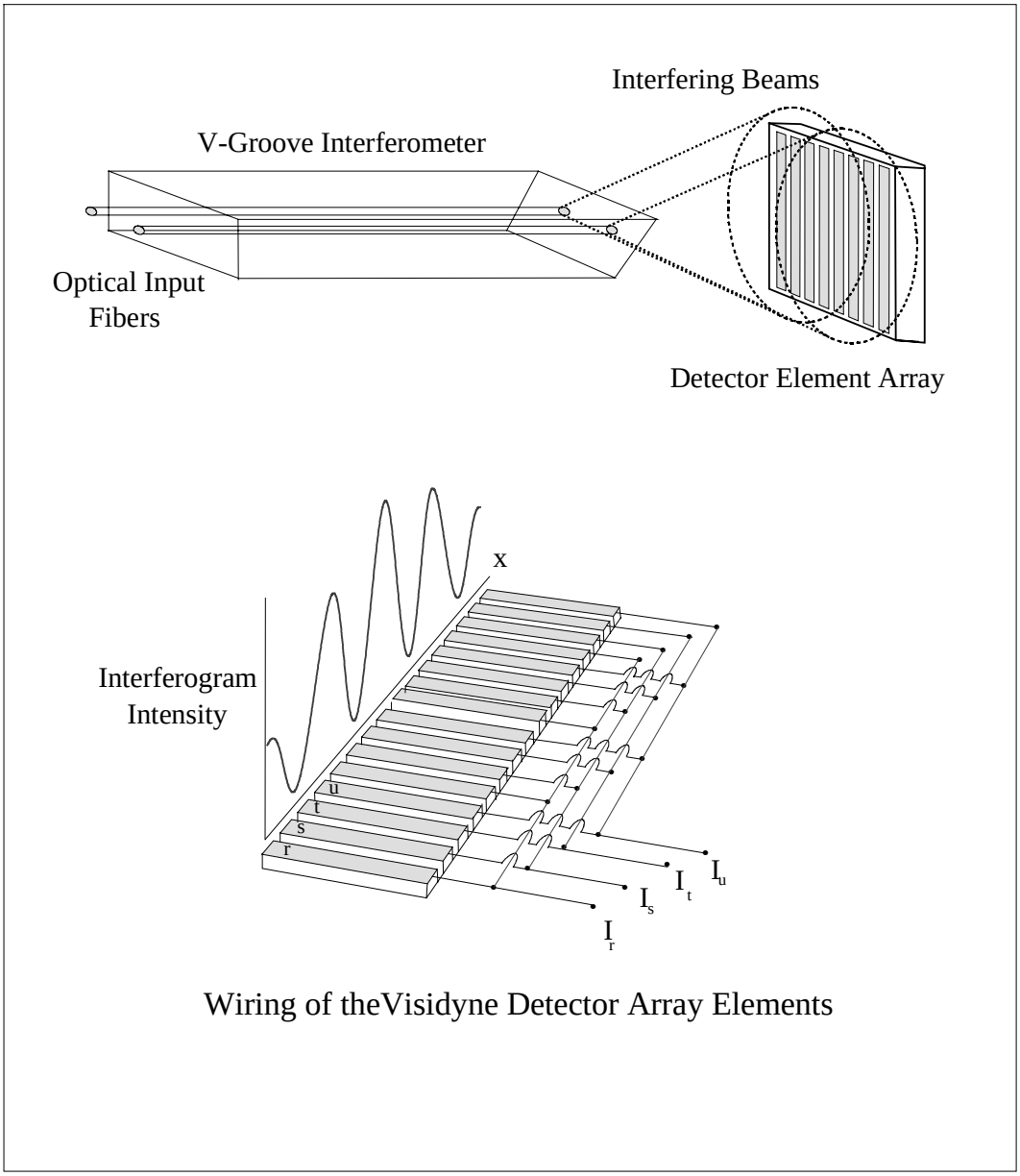

Figure 2: The Visidyne Interferometer

Precision High Resolution Phase Recovery

It is critical to the success of the design to recover the phase $\phi(t) = G(t)\cdot V/V_\pi$ between the two beams at some fundamental, shotnoise or detector noise limit at large bandwidth (>10 MHz) and with a high degree of precision, linearity, and DC stability. At Visidyne we determine the optical phase interferometrically by projecting the two optical outputs of relative phase, $\phi(t)$, onto a detector array (see Figure 2). The two optical outputs make a spatial fringe pattern, the change in position of which is linearly related to $\phi(t)$. As the optical phase changes, the fringe pattern shifts along the detector plane. The position of the fringe pattern is therefore linearly related to the voltage applied to the waveguide modulator. The position of the spatial fringe pattern is calculated by sampling the spatial fringe pattern at ¼ spatial wavelengths. This is done by interleaving the groups of 4 detectors and summing the results (see Figure 2) producing the following signals,

$$I_R = I_{DC} + I_A(\cos 2\pi\phi(t) + 0) + I_N \qquad I_S = I_{DC} + I_A(\cos 2\pi\phi(t) + 1/4) + I_N$$

$$I_T = I_{DC} + I_A(\cos 2\pi\phi(t) + 1/2) + I_N \qquad I_U = I_{DC} + I_A(\cos 2\pi\phi(t) + 3/4) + I_N$$

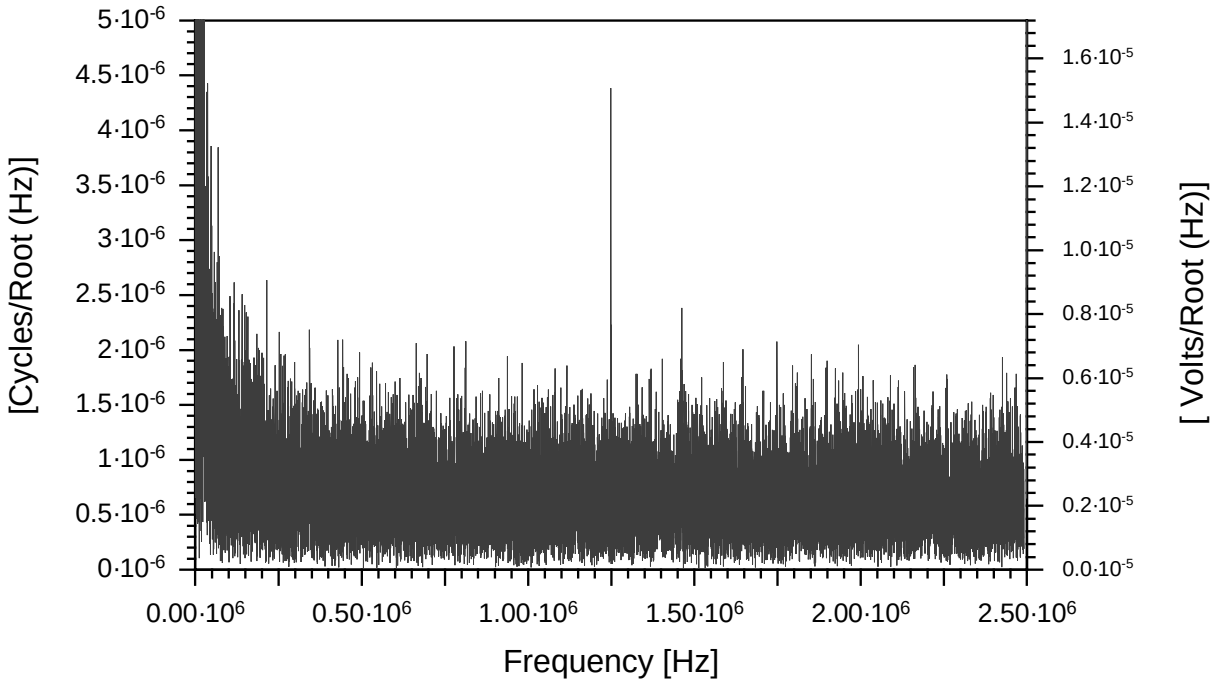

Figure 3: The Cryolink Noise Spectrum

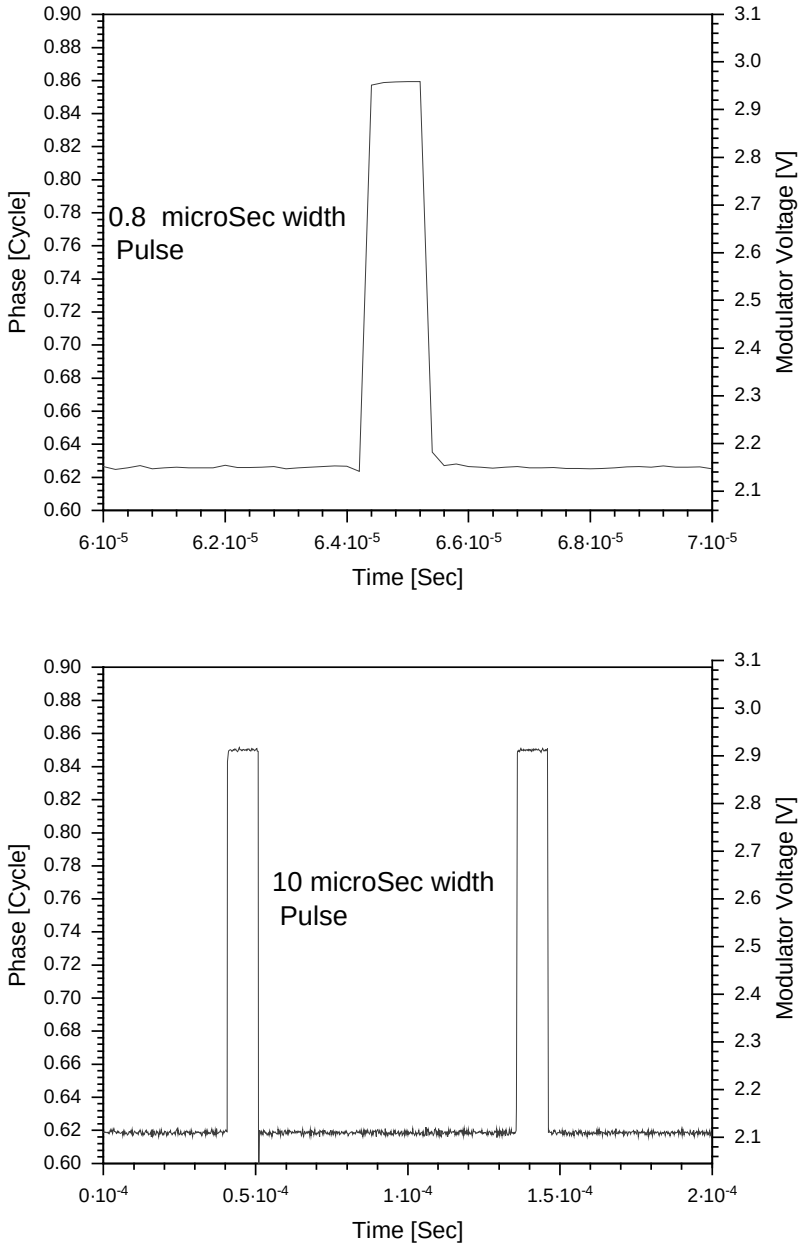

Figure 4: Example of Cryolink Transmitted Transient Data

where I_R, I_S, I_T and I_U correspond to 90° intervals of spatial fringe sampling, I_{DC} is a common DC brightness level and I_{AC} a common AC amplitude, proportional to interference fringe visibility and I_N is added noise. One way to solve for the phase, $\phi(t)$, is to arrange them as two quadrature signals,

$$I_X = I_R - I_T \qquad I_Y = I_S - I_U$$

The two signals, $I_X(t)$ and $I_Y(t)$, after being digitized to e.g., 13 bits are applied to a high speed > 20 MHz coordinate transformation chip. The chip then computes the instantaneous phase up to a resolution of 13 bits using an arc tangent transformation and a high speed look-up table equivalent to $\phi(t) = \tan^{-1} I_Y(t)/I_X(t)$, Due to the ratiometric nature of this process the effect of any added laser intensity noise I_N is then cancelled and remains unaffected by temperature and operating point while having excellent resolution and bandwidth capability.

The encoding of the signal as phase modulation introduces a problem, which does not exist when the intensity modulation method is employed. Since the exit fibers are part of the interferometer, any path differences between the fibers e.g., due temperature, pressure, vibration manifest themselves as equivalent signals or phase errors. As the least significant bit may represent a phase shift of $1/2^{13}$ cycles or a path difference of $\lambda/2^{13}$ = 0.1 nm, the two fiber lengths should be kept to a relative difference to fractions of a nanometer. For the case e.g. of 3 meters of fiber length a relative, differential stability of $1/2^{13}$ which would appear to be a formidable challenge. In practice, as will be shown, the required degree of stability can be realized over the period of a video frame e.g. 10 to 30 msec.

A number of factors contribute to optical fiber length stability. First, the optical fibers are made of the highly homogeneous material, fused silica and therefore have very predictable effects with temperatures and pressure. When the two optical fibers are packaged in close proximity, a high degree of common mode rejection to environmental influences results. For example, a single fiber's optical path length changes by 17 cycles/ m °C, two bundled fibers have a *differential* optical path difference is reduced to 0.5 cycles/meter °C. Secondly, since any drift due is only important as it occurs over a period of a frame, drift rates per frame of < 10^{-4} cycle are then readily attainable as temperature changes greater than 0.1 °C/sec are unlikely in a normal environment such as a satellite.

Other Sources of Error

There are a number of sources of error, random noise and systematic, which may affect the performance of the Cryolink optical readout. Random sources include detection/preamp, thermal and shot noise statistics as well as quantization errors of the A/D and phase processor. A number of noise sources associated with unintentional phase changes may also occur.

As already discussed, systematic errors due to the thermo-mechanical strain in the exit fibers may create a path difference between the two optical fibers. Or the laser diode wavelength may drift due to a temperature/current change. Small errors associated with non-uniformities between pixel sensitivity, as

well as mismatch between the pitch of the interferometer fringe pattern and the detector spacing array may also occur. Additionally, computational errors in the phase processor are present in the calculation of the phase. These errors can be collectively described as φ_{tot} , expressed in cycles or as an equivalent input noise voltage, $e_t = (\varphi_{tot}\ V_\pi)/G$,

$$\varphi_{tot} = \frac{1}{m_e}\left(\frac{2eB}{R_I P_d}\right)^{1/2} + \frac{1}{2^{(n-1)}} + \frac{ds}{dT}\frac{dT}{dt}\Delta l t_{frame}\sigma + \frac{d\sigma}{dt}\Delta l t_{frame} + \varepsilon_{\det} + \varepsilon_{proc}$$

The first term on the right is the detector shot noise component where $e = 1.6 \times 10^{-19}$ *C, B* the detector/preamp bandwidth (5 MHz), R_I the detector response (0.6 A/Watt) and P_d the detector power and m_e is the modulation efficiency of the interferometer. Due to the finite width of the detector elements, m_e = 0.7. For $P_d \geq 1$ *mW,* the detector shot noise dominates, $\varphi_{tot} = 5 \times 10^{-5}$ cycles.

The second term is associated with the quantification noise of the processor. For full scale e.g. ±5 Volts signal, the phase resolution of the processor is $\geq 1/2^{13} = 10^{-4}$ *cycles.* The third term represents the influence a temperature drift on the differential optical path length of the paired fibers. Assuming a change in the thermo-mechanical strain, $ds/dT = 1.5\ 10^{-5}$ *[cycles/°C m],* and fiber pair matched to a length, $\Delta l = 1$ *mm*, temperature drift rate of $dT/dt = 0.1$ *°C/sec,* a wavelength of $\sigma = 1/\lambda = 12{,}000\ cm^{-1}$, and IRFPA frame rate of e.g. 100 frames/sec, $t_{frame} = 10$ *msec,* $\Delta\varphi(t)$ will result in a total phase error of 1.8×10^{-7} cycles.

The fourth term represents the phase drift due to a wavelength change rate of $d\sigma/dt \cdot dl$. With even a minimal laser diode temperature control, phase drift is negligible. The last two terms, describing the detector and processor noise, $\varepsilon_{\det}$ and ε_{proc} each are will below $< 10^{-4}$ cycle.

Experimental Demonstration

A measure of the Cryolink equivalent input noise was made by applying a 1500 Hz signal to the optical transducer. The transmitted signal was recorded and a spectrum analysis was performed. As can be seen in Figure 3, the noise level is nearly white with only a slight increase below 100 kHz, reaching a value of $7 \cdot 10^{-7}$ Volts/√Hz for most of the 2.5 MHz bandwidth. The main spectral component at 1500 Hz, not visible in this plot, was measured to have a value of 1.7 Volts. Since the total noise is approximately equal to the baseline noise level of $7 \cdot 10^{-7}$ Volts/√Hz · √(2.5 MHz bandwidth), a signal-to noise ratio (SNR) of $1.7/(1.1\ 10^{-3}) \cong 1500$ was calculated. The low noise characteristics of the Cryolink system are also evident when viewed in the time domain. A test of the digital transmission capabilities were performed by applying a series of *10* and *0.8 μsec* pulses to the waveguide modulator (see Figure 4). The sub-microsecond response of the Cryolink system to the pulses is clearly visible in the transmitted data as well as a large SNR.

Various qualitative image tests of the Cryolink system were performed and are presented in the Figures 5, 6 and 7. The results of the first test are shown in Figure 5, which displays a “frame grabbed” IR Amber camera video frame after Cryolink transmission. Evidently, no apparent degradation to the 128 X 256 pixel image was introduced by the Cryolink system when compared to the identical frame as recorded directly from the Amber camera.

The test was repeated using the higher resolution video Pulnix camera to generate an image of a test pattern consisting of dashes and dots ranging from 1 to 32 pixels image in size. The test pattern of the Cryolink transmitted image (Figure 6) compares very well with the direct camera output image. Line quality remains straight and dots remain visible to nearly the single pixel size.

Finally a video of our sponsor logo (AFRL) (Figure 7) was transmitted and recorded. A slight herring bone pattern is evident in the recorded which has been traced to the 10 MHz sampling timing signal required by the digitizing circuitry. Reduction in this noise pattern will come with improved filtering techniques and change to a printed circuit construction from the current brassboard construction.

Acknowledgments

The work presented here has had a long gestation period with many individuals providing crucial and timely support. They include Dr. Thomas Cunningham of the Jet Propulsion Laboratory, who defined the original requirements for the fiber optic readout and who forced us to address some important technical issues. Mr. David Cardimona of the Air Force Research Laboratory (AFRL) who early on appreciated its potential and Dr. Paul LeVan of the AFRL and Dr. Marc Wigdor of the Nichols Research Co. who saw its utility for the Air Force and BMDO missions. Appreciation also goes to Mr. Robert Hancock of the AFRL-SBIR office; his initiative and imagination made it possible to graft on the Air Force contract onto an effort that had a NASA origin.

References

1. Private conversation with Dr. Paul LeVan of AFRL, Albuquerque, NM
2. Briefing Material from SBIRS LOW Day, 1 May, 1997.- Dr. O. Milton, USA, SSDC
3. Superconductors for IR Imaging, AV Week April 20, 1998, page 60
4. Private conversation , Dr. Thomas Cunningham of JPL
5. Hyde et al., IRFPA Optical Interface, Proceedings, SPIE, Vol. 2226 (1993)
6. Johnston et al. Optical Links for Cryogenic Focal Plane Array Readout, Optical Engineering, 33, (6) – 2013-2019, June 1994

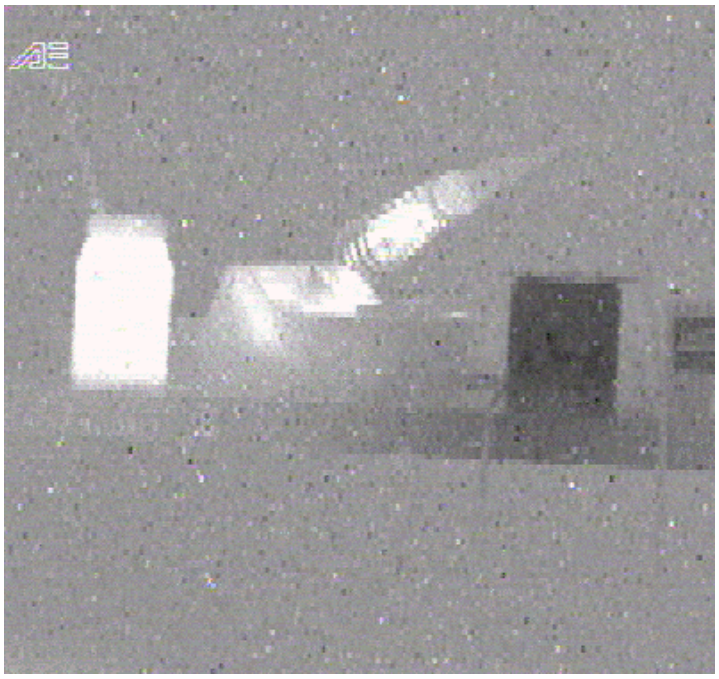

128 X 256 Cryolink Transmitted IR Video Image

Figure 5: The Same Image Direct to Frame Grabber

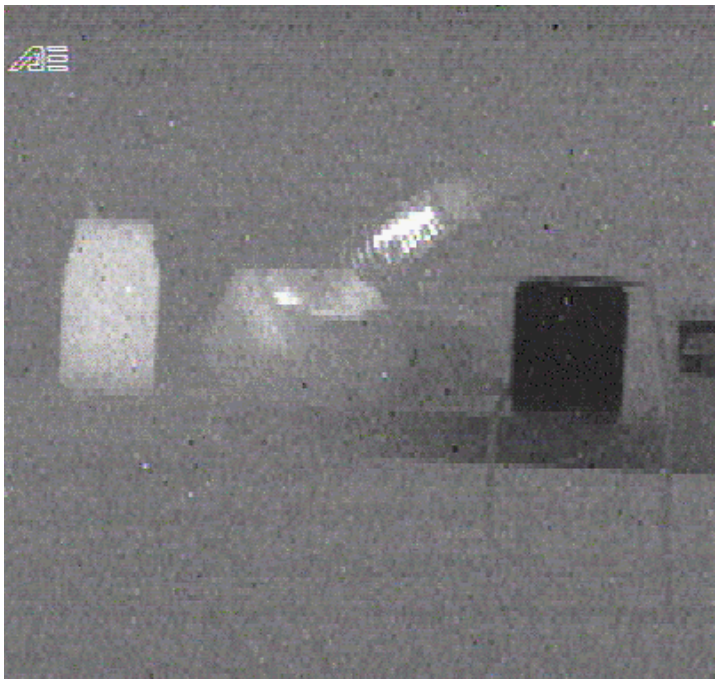

A 640 X 480 Cryolink Transmitted Image

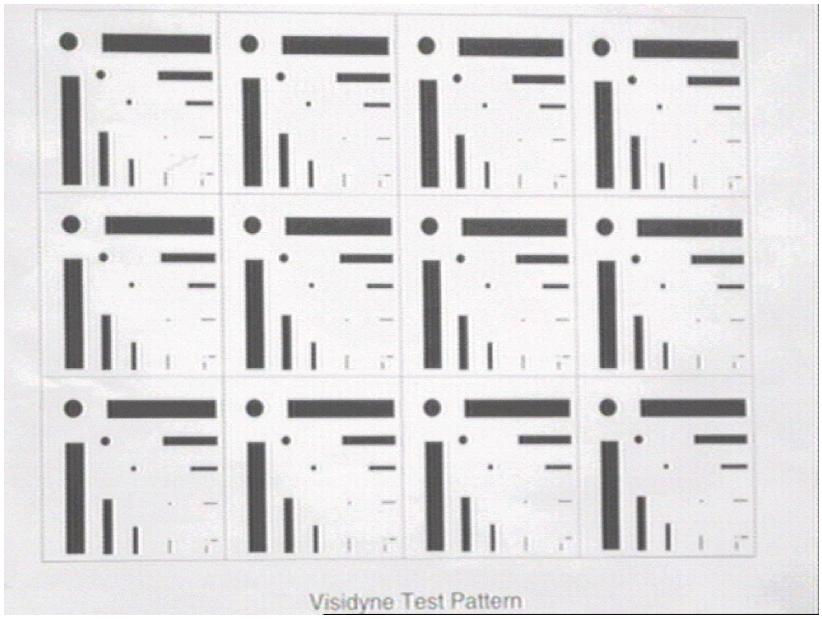

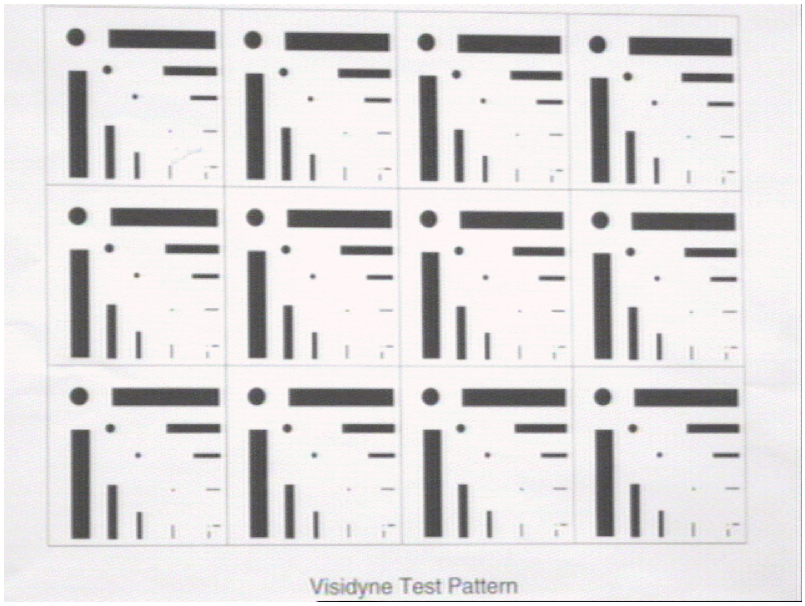

Figure 6: The Same Image Direct to Frame Grabber

Figure 7: A Video Image of our Sponsor's Logo